

Electronic Structure and Doping of P-Type Transparent Conducting Oxides

Preprint

S.-H. Wei, X. Nie, and S.B. Zhang

*To be presented at the 29th IEEE PV Specialists
Conference
New Orleans, Louisiana
May 20-24, 2002*



NREL

National Renewable Energy Laboratory

1617 Cole Boulevard
Golden, Colorado 80401-3393

NREL is a U.S. Department of Energy Laboratory
Operated by Midwest Research Institute • Battelle • Bechtel

Contract No. DE-AC36-99-GO10337

NOTICE

The submitted manuscript has been offered by an employee of the Midwest Research Institute (MRI), a contractor of the US Government under Contract No. DE-AC36-99GO10337. Accordingly, the US Government and MRI retain a nonexclusive royalty-free license to publish or reproduce the published form of this contribution, or allow others to do so, for US Government purposes.

This report was prepared as an account of work sponsored by an agency of the United States government. Neither the United States government nor any agency thereof, nor any of their employees, makes any warranty, express or implied, or assumes any legal liability or responsibility for the accuracy, completeness, or usefulness of any information, apparatus, product, or process disclosed, or represents that its use would not infringe privately owned rights. Reference herein to any specific commercial product, process, or service by trade name, trademark, manufacturer, or otherwise does not necessarily constitute or imply its endorsement, recommendation, or favoring by the United States government or any agency thereof. The views and opinions of authors expressed herein do not necessarily state or reflect those of the United States government or any agency thereof.

Available electronically at <http://www.osti.gov/bridge>

Available for a processing fee to U.S. Department of Energy
and its contractors, in paper, from:

U.S. Department of Energy
Office of Scientific and Technical Information
P.O. Box 62
Oak Ridge, TN 37831-0062
phone: 865.576.8401
fax: 865.576.5728
email: reports@adonis.osti.gov

Available for sale to the public, in paper, from:

U.S. Department of Commerce
National Technical Information Service
5285 Port Royal Road
Springfield, VA 22161
phone: 800.553.6847
fax: 703.605.6900
email: orders@ntis.fedworld.gov
online ordering: <http://www.ntis.gov/ordering.htm>



Printed on paper containing at least 50% wastepaper, including 20% postconsumer waste

ELECTRONIC STRUCTURE AND DOPING OF P-TYPE TRANSPARENT CONDUCTING OXIDES

Su-Huai Wei, Xiliang Nie, and S. B. Zhang
National Renewable Energy Laboratory, Golden, CO 80401, U.S.A.

ABSTRACT

Transparent conducting oxides (TCOs) are a group of materials that are widely used in solar cells and other optoelectronic devices. Recently, Cu-containing p-type TCOs such as $M^{II}Cu_2O_2$ ($M^{II} = \text{Mg, Ca, Sr, Ba}$) and $CuM^{III}O_2$ ($M^{III} = \text{Al, Ga, In}$) have been proposed. Using first-principles band structure methods, we have systematically studied the electronic and optical properties of these p-type transparent oxides. For $M^{II}Cu_2O_2$, we predict that adding a small amount of Ca into $SrCu_2O_2$ can increase the transparency and conductivity. For $CuM^{III}O_2$, we explained the doping and band gap anomalies in this system and proposed a new approach to search for bipolar dopable wide-gap materials.

INTRODUCTION

Transparent conducting oxides (TCOs) are materials that are widely used in solar cells and other optoelectronic devices [1]. Almost all of the well-known TCOs, such as ZnO , In_2O_3 , SnO_2 , and their alloys, have n-type conductivity. The lack of p-type TCOs has severely limited the potential applications of these materials. Consequently, considerable efforts have been devoted to develop p-type TCOs and to understand the doping mechanism in these materials [2-7].

Recently, several Cu-containing p-type TCOs such as $SrCu_2O_2$ and $CuM^{III}O_2$ ($M^{III} = \text{Al, Ga, In}$) have been proposed [2,5-7]. The idea is based on the observations that Cu has shallow, occupied $3d$ orbital that is close to the O $2p$ orbitals. The coupling between the Cu d states and the O p states can lead to smaller ionization energies (which is equivalent to higher VBM) for these Cu compounds than for conventional oxides, thus, making it easier to dope them p-type.

Besides showing p-type conductivity, these materials also show some unique and unexplained physical properties [5-7]. For example, the optically *measured* direct band gap increases from 3.5 eV ($CuAlO_2$), to 3.6 eV ($CuGaO_2$), and to 3.9 eV ($CuInO_2$). This trend is

in sharp contrast to the trend found in other group III containing semiconductors, in which the band gap decreases as the atomic number of the group III elements increases [8]. Furthermore, bipolar doping is achieved, but only in $CuInO_2$ by extrinsic dopants [7]. This is quite puzzling because $CuInO_2$ has the largest reported band gap [7]. No similar trend has ever been observed in any other semiconductors.

We have systematically studied the electronic and optical properties of these p-type transparent oxides. For $M^{II}Cu_2O_2$ ($M^{II} = \text{Mg, Ca, Sr, Ba}$), the trend of band gap variation of $M^{II}Cu_2O_2$ as a function of M^{II} is explained in terms of atomic energy levels and atomic sizes of the M^{II} elements. For $SrCu_2O_2$, the calculated effective masses for the conduction band states are found to be larger than those for the valence states, opposite to the trend in conventional semiconductors and n-type TCOs. We predict that adding a small amount of Ca into $SrCu_2O_2$ can increase the band gap and reduce the hole effective mass of $SrCu_2O_2$, therefore, increase the transparency and conductivity. For $CuM^{III}O_2$, we show that the doping and band gap anomalies in this system are results of a large disparity between the fundamental gap and the apparent optical gap, a finding that could lead to breakthroughs towards bipolarly dopable wide-gap semiconductor oxides.

METHOD OF CALCULATION

The band structure calculations were performed using the first-principles local density approximation (LDA) as implemented by the general potential linearized augmented plane wave (LAPW) method [9]. We used the Ceperley-Alder exchange correlation potentials as parameterized by Perdew and Zunger [10]. The Ca $3p$, Sr $4p$, and Ba $5p$ states, as well as the Ga $3d$ and In $4d$ states, are treated as valence states. Spin-orbit coupling is included when calculating the effective mass. The optical properties of these materials are studied by calculating the dipole momentum matrix element $P_{i,j}(\mathbf{k}) = |\langle \psi_{i,\mathbf{k}} | \mathbf{P} | \psi_{j,\mathbf{k}} \rangle|^2$ and the absorption coefficient using the optic package in WIEN97 code [11].

RESULTS AND DISCUSSIONS

$M^{II}\text{Cu}_2\text{O}_2$

$M^{II}\text{Cu}_2\text{O}_2$ has the tetragonal crystal structure with space group of $I4_1/amd$ (Fig. 1b). In this crystal structure, M^{II} atoms are at the center of a distorted octahedron formed by O atoms. The Cu atoms form the well-known O-Cu-O dumbbell configuration, which is similar to that of Cu_2O (Figure 1a). In fact, $M^{II}\text{Cu}_2\text{O}_2$ can be considered as being derived from Cu_2O_2 , in which one Cu atom is removed for each unit of distorted Cu_2O , plus an inter-penetrating body-centered tetragonal Sr sublattice.

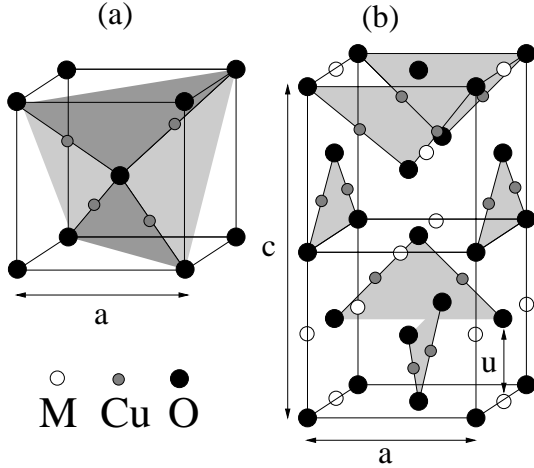


Fig. 1. Crystal structure of (a) Cu_2O and (b) $M^{II}\text{Cu}_2\text{O}_2$.

The calculated band structure of SrCu_2O_2 at the experimental lattice constants along some high symmetry directions is shown in Fig. 2c. It shows that SrCu_2O_2 has a direct band gap at Γ . Analysis of the electron density of states (DOS) [3] for SrCu_2O_2 indicates that the valence states consist of two major parts. The upper part from the valence band maximum (VBM) to $E_{\text{VBM}} - 3$ eV consists predominantly of the Cu $3d$ states. The lower part from $E_{\text{VBM}} - 3$ eV to $E_{\text{VBM}} - 6$ eV consists predominantly of the O $2p$ states. This is due to the fact that Cu $3d$ level is shallower than O $2p$. Thus, the Cu-containing oxides such as Cu_2O have much higher VBM than other conventional oxides such as ZnO , where the Zn $3d$ state is deeper than the O $2p$ state. Higher VBM also leads to higher p-type dopability, as suggested by the doping limit rule [12]. Comparing to Cu_2O , we find that adding SrO into Cu_2O reduces the $d-d$ coupling between the Cu atoms and raises the band gap by 1.31 eV, in good agreement with the experimental value of 1.22 eV.

In order to be transparent, a p-type TCO not only should have a large fundamental band gap, so no visible light absorption between the valence bands and

the conduction bands can take place, but also should have no visible light absorption between the VBM and the bands below. We have calculated the momentum transition matrix elements between the VBM state and other states at Γ [3]. We find that, indeed, the dipole transition probabilities between the VBM and states within 4 eV below the VBM are negligible. This is because the on-site transition from the same angular momentum (such as O p to O p and Cu d to Cu d) is forbidden according to the classical selection rule. This explains the transparency for this p-type material.

A p-type TCO with good conductivity should also have high mobility, and thus, small hole effective mass. To test this, the electron and hole effective masses for the tetragonal SrCu_2O_2 are calculated along high symmetry lines parallel or perpendicular to the c directions. The results are shown in Table I. We find that for this p-type material, the effective mass of the conduction band minimum (CBM) is much larger than that of the VBM. Both the electron effective masses and the hole effective masses are anisotropic. The hole effective masses along the c -axis are much larger than the one perpendicular to the c axis. These results indicate that for single crystal, which could be obtained by epitaxial growth, hole conductivity perpendicular to the c -axis will be much larger than that parallel to the c -axis.

To search for better p-type TCOs we have also calculated the band structures of $M^{II}\text{Cu}_2\text{O}_2$ with $M=\text{Mg}$, Ca, Sr, and Ba. The calculated band structures are plotted in Fig. 2. All the four compounds show direct band gaps at Γ with $E_g = 2.45, 3.01, 3.33, 3.30$ eV, respectively, after the LDA correction [3]. We see that the variation of the band gaps of $M^{II}\text{Cu}_2\text{O}_2$ is non-monotonic. The band gaps increase from MgCu_2O_2 to CaCu_2O_2 to SrCu_2O_2 , but becomes smaller when Sr is replaced by Ba. This trend of band gap variation of $M^{II}\text{Cu}_2\text{O}_2$ as a function of M^{II} can be understood by noticing that there are several states near the valence and conduction band edges, and each state has different dependence on atomic energy levels and volume deformation potentials [3]. The non-monotonic behavior is due to band crossing at the band edge: MgCu_2O_2 , CaCu_2O_2 , and SrCu_2O_2 all

Table I. Calculated effective masses (in m_0) of SrCu_2O_2 at Γ along high symmetry lines parallel (\parallel) or perpendicular (\perp) to the c directions. The results are calculated with spin-orbit coupling at experimental lattice constants. The states are labeled using semi-relativistic notations.

States	m_{\perp}	m_{\parallel}
Γ_2	2.40	0.44
Γ_5	0.48	2.12
	0.57	1.27
Γ_1	5.85	1.82
Γ'_1	0.32	0.79
Γ'_3	0.28	0.44

have the Γ_5 VBM state, whereas the VBM of BaCu_2O_2 is a Γ_2 state. Similarly, MgCu_2O_2 and CaCu_2O_2 have the Γ'_3 CBM state and SrCu_2O_2 has the Γ_1 CBM state, whereas the CBM of BaCu_2O_2 has the Γ'_1 symmetry.

We have also calculated the electron and hole effective masses at Γ for states near the band edge of the $\text{M}^{II}\text{Cu}_2\text{O}_2$ compounds. We find that, in general, all the $\text{M}^{II}\text{Cu}_2\text{O}_2$ compounds have similar effective masses as for SrCu_2O_2 . Both the electron and hole effective masses are anisotropic. The hole effective masses perpendicular to c directions at VBM are relatively small for MgCu_2O_2 , CaCu_2O_2 , and SrCu_2O_2 . Due to O-mediated coupling between Cu d states, the effective masses also decrease when the unit cell volumes decrease from SrCu_2O_2 to CaCu_2O_2 to MgCu_2O_2 .

Our calculated results show that for pure $\text{M}^{II}\text{Cu}_2\text{O}_2$, SrCu_2O_2 has the largest band gap, thus is likely to be the most transparent. The band gap could be increased slightly if a fraction of Ca ($x \sim 16\%$) is mixed into SrCu_2O_2 to form $(\text{Ca}_x\text{Sr}_{1-x})\text{Cu}_2\text{O}_2$ alloys. Furthermore, our calculations show that due to larger $p-d$ and $d-d$ couplings in CaCu_2O_2 , its VBM is also slightly higher in energy (~ 0.1 eV) than the VBM of SrCu_2O_2 . Based on the doping limit rule [12], CaCu_2O_2 should also be easier to dope p-type than SrCu_2O_2 . Therefore, we predict that adding a small amount of Ca into SrCu_2O_2 can increase both the transparency and conductivity.

$\text{CuM}^{III}\text{O}_2$

$\text{CuM}^{III}\text{O}_2$ has a layered delafossite crystal structure with the space group of $R\bar{3}m$. It is composed of O-Cu-O dumbbell layers in a hexagonal plane separated by an M^{III}O_6 edge-sharing octahedra layer (see Fig. 3).

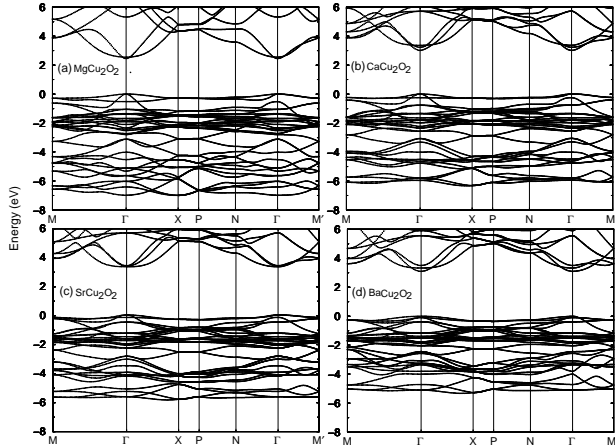


Fig. 2. Calculated electronic band structure for (a) MgCu_2O_2 , (b) CaCu_2O_2 , (c) SrCu_2O_2 , and (d) BaCu_2O_2 . Energy zero is at VBM. The energy of the conduction bands are shifted upward by 1.5 eV to correct the LDA band gap error.

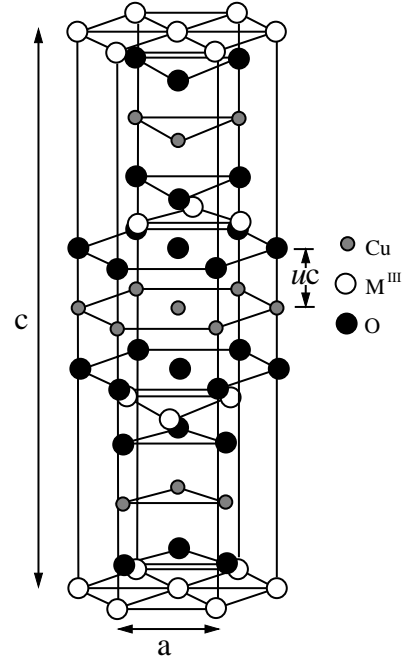


Fig. 3. The crystal structure of delafossite compounds $\text{CuM}^{III}\text{O}_2$.

The calculated band structures at experimental lattice constants for $\text{CuM}^{III}\text{O}_2$ ($\text{M}=\text{Al}$, Ga , and In) are shown in Fig. 4. The following general trends are observed:

(i) All three compounds have indirect fundamental band gaps with the CBM at Γ and the VBM on the Γ -F line near F, as indicated by the black circles in Fig. 4. The LDA-calculated indirect gaps are 1.97, 0.95, and 0.41 eV, respectively, for CuAlO_2 , CuGaO_2 , and CuInO_2 .

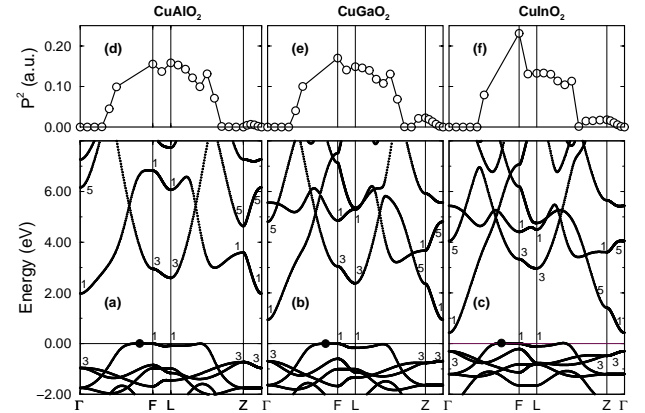


Fig. 4. (a) to (c) are the calculated LDA band structures for CuAlO_2 , CuGaO_2 , and CuInO_2 , respectively. Energy zero is at the highest valence band at F. The VBMs are marked by the black circles. (d) to (f) are the corresponding transition matrix elements between the band edge states. The LDA band gap error of ~ 0.8 eV is not added in this plot.

(ii) The direct band gap at Γ decreases considerably from 2.93 for CuAlO_2 , to 1.63 for CuGaO_2 , to 0.73 for CuInO_2 . It also decreases at Z from 4.32 to 3.12 to 1.89 eV. This is consistent with the trend in other group III containing semiconductors. The decrease of the band gap from Al to Ga to In is mainly an atomic size effect: the CBM states at Γ_{1c} and Z_{1c} (or Z_{5c}) have significant antibonding s character. As the volume increases from the Al to Ga to In compounds, the energies of the antibonding states are lowered.

(iii) The direct band gap at F increases from 2.95 for CuAlO_2 , to 3.05 for CuGaO_2 , and to 3.34 for CuInO_2 . A similar trend is observed at L: it decreases slightly from 2.68 for CuAlO_2 to 2.54 for CuGaO_2 , then increases to 3.08 eV for CuInO_2 . The increase of the gap at F (L) from Al or Ga to In is also a size effect. The conduction band edge states F_{3c} and L_{3c} have most of their charge densities in the interstitial region. Thus when the volume increases, the energy levels of F_{3c} and L_{3c} also increase.

The experimentally observed optical gaps increase from 3.5 (CuAlO_2), to 3.6 (CuGaO_2), to 3.9 eV (CuInO_2). This trend clearly contradicts the trend in the calculated fundamental direct gaps of 2.68 eV (L) for CuAlO_2 , 1.64 eV (Γ) for CuGaO_2 , and 0.73 eV (Γ) for CuInO_2 , showing a decrease. To resolve this discrepancy, we have calculated the matrix elements for direct transitions between band edge states. The upper panel of Fig. 4 shows the results for CuAlO_2 , CuGaO_2 , and CuInO_2 at the Γ , F, L, and Z points and in between. It reveals that direct transitions between Γ_{3v} and Γ_{1c} , and between Z_{3v} and Z_{1c} , are forbidden in the delafossite structure because both states have the same (even) parity. An important consequence is that absorption *near* the fundamental gap at Γ for CuGaO_2 and CuInO_2 is very small and barely increases with energy until transitions at the next critical point take place (which define an apparent optical band gap). The calculated apparent gap [4] is very much unchanged from CuAlO_2 to CuGaO_2 , but increases by +0.4 eV from CuAlO_2 to CuInO_2 , in good agreement with experiment. The large differences in terms of the energy and transition matrix element between the fundamental direct gap and the apparent gap are the reason for the band gap anomalies seen in $\text{CuM}^{III}\text{O}_2$.

The p-type conductivity of $\text{CuM}^{III}\text{O}_2$ and the mysterious bipolar dopability of CuInO_2 can also be understood within the framework of equilibrium doping theory. According to the recently developed “doping limit rule” [12], the degree of self-compensation in a material correlates directly to its band edge positions with respect to others. A compound with higher VBM is easier to dope p-type, whereas a compound with lower CBM is easier to dope n-type. Our calculated band alignments [4] between the $\text{CuM}^{III}\text{O}_2$ show that the valence band offsets for this common-anion system are rather small. The VBMs for CuGaO_2 and CuInO_2 is

about 0.17 eV higher than that for CuAlO_2 as a result of the coupling between the group III d orbitals and the O p orbital. Hence, p-type conductivity might be slightly easier to reach in CuGaO_2 and CuInO_2 than in CuAlO_2 . However, the VBM for CuGaO_2 is 0.8 eV higher than ZnO, which explains why $\text{CuM}^{III}\text{O}_2$ can be made into p-type TCOs, whereas it is difficult to achieve p-type ZnO. On the other hand, due to a large volume deformation, the CBM of CuInO_2 is 1.48 eV lower than CuAlO_2 . This explains why n-type conductivity can also be achieved in this nominally p-type material. Thus, a low CBM combined with a large apparent gap explains the puzzling combination of good transparency with bipolar dopability in CuInO_2 . This finding provides a new avenue to achieving bipolar doping in wide-gap materials.

ACKNOWLEDGMENTS

This work was supported in part by U.S. Department of Energy, Grant DE-AC36-99-GO10337.

REFERENCES

- [1] See Reviews in MRS Bull. **25**, (2000).
- [2] H. Kawazoe, M. Yasukawa, H. Hyodo, M. Kurita, H. Yanagi, and H. Hosono, Nature (London) **389**, 939 (1997).
- [3] X. Nie, S.-H. Wei, and S. B. Zhang, Phys. Rev. B **65**, 075111 (2002).
- [4] X. Nie, S.-H. Wei, and S. B. Zhang, Phys. Rev. Lett. **88**, 066405 (2002).
- [5] H. Yanagi, S. Inoue, K. Ueda, and H. Kawazoe, J. App. Phys. **88**, 4159 (2000).
- [6] K. Ueda, T. Hase, H. Yanagi, H. Kawazoe, H. Hosono, H. Ohta, M. Orita, and M. Hirano, J. App. Phys. **89**, 1790 (2001).
- [7] H. Yanagi, T. Hase, S. Ibuki, K. Ueda, and H. Hosono, App. Phys. Lett. **78**, 1583 (2001).
- [8] *Landolt-Bornstein: Numerical Data and Functional Relationships in Science and Technology*, Group III, Vol. 22a, edited by O. Madelung and M. Schulz, (Springer-Verlag, Berlin, 1987).
- [9] S.-H. Wei and H. Krakauer, Phys. Rev. Lett. **55**, 1200 (1985), and references therein.
- [10] J. P. Perdew and A. Zunger, Phys. Rev. B **23**, 5048 (1981).
- [11] R. Abt, C. Ambrosch-Draxl, and P. Knoll, Physica B **194-196**, 1451 (1994).
- [12] S. B. Zhang, S.-H. Wei, and A. Zunger, J. Appl. Phys. **83**, 3192 (1998).

REPORT DOCUMENTATION PAGE			Form Approved OMB NO. 0704-0188	
Public reporting burden for this collection of information is estimated to average 1 hour per response, including the time for reviewing instructions, searching existing data sources, gathering and maintaining the data needed, and completing and reviewing the collection of information. Send comments regarding this burden estimate or any other aspect of this collection of information, including suggestions for reducing this burden, to Washington Headquarters Services, Directorate for Information Operations and Reports, 1215 Jefferson Davis Highway, Suite 1204, Arlington, VA 22202-4302, and to the Office of Management and Budget, Paperwork Reduction Project (0704-0188), Washington, DC 20503.				
1. AGENCY USE ONLY (Leave blank)		2. REPORT DATE May 2002		3. REPORT TYPE AND DATES COVERED 29 th IEEE PVSC-Conference Paper May 20-24 2002
4. TITLE AND SUBTITLE Electronic Structure and Doping of P-Type Transparent Conducting Oxides: Preprint				5. FUNDING NUMBERS PVP22401
6. Author(S) S.-H. Wei, X. Nie, and S.B. Zhang				
7. PERFORMING ORGANIZATION NAME(S) AND ADDRESS(ES) National Renewable Energy Laboratory 1617 Cole Blvd. Golden, CO 80401-3393				8. PERFORMING ORGANIZATION REPORT NUMBER
9. SPONSORING/MONITORING AGENCY NAME(S) AND ADDRESS(ES) National Renewable Energy Laboratory 1617 Cole Blvd. Golden, CO 80401-3393				10. SPONSORING/MONITORING AGENCY REPORT NUMBER NREL/CP-520-32199
11. SUPPLEMENTARY NOTES				
12a. DISTRIBUTION/AVAILABILITY STATEMENT National Technical Information Service U.S. Department of Commerce 5285 Port Royal Road Springfield, VA 22161				12b. DISTRIBUTION CODE
13. ABSTRACT (<i>Maximum 200 words</i>): Transparent conducting oxides (TCOs) are a group of materials that are widely used in solar cells and other optoelectronic devices. Recently, Cu-containing p-type TCOs such as $M^{II}Cu_2O_2$ ($M^{II}=Mg, Ca, Sr, Ba$) and $CuM^{III}O_2$ ($M^{III}=Al, Ga, In$) have been proposed. Using first-principles band structure methods, we have systematically studied the electronic and optical properties of these p-type transparent oxides. For $M^{II}Cu_2O_2$, we predict that adding a small amount of Ca into $SrCu_2O_2$ can increase the transparency and conductivity. For $CuM^{III}O_2$, we explained the doping and band gap anomalies in this system and proposed a new approach to search for bipolar dopable wide-gap materials.				
14. SUBJECT TERMS: PV; transparent conducting oxides (TCOs); optoelectronic devices; bandgap anomalies; linearized augmented plane wave (LAPW); spin-orbit coupling; crystal structure;				15. NUMBER OF PAGES
				16. PRICE CODE
17. SECURITY CLASSIFICATION OF REPORT Unclassified		18. SECURITY CLASSIFICATION OF THIS PAGE Unclassified		19. SECURITY CLASSIFICATION OF ABSTRACT Unclassified
				20. LIMITATION OF ABSTRACT UL